ELSEVIER

Journal of Applied Geophysics 45 (2000) 1–18

JOURNAL OF APPLIED GEOPHYSICS

www.elsevier.nl/locate/jappgeo

Improvement in TDEM sounding interpretation in presence of induced polarization. A case study in resistive rocks of the Fogo volcano, Cape Verde Islands

Marc Descloitres [a,*], Roger Guérin [b], Yves Albouy [a], Alain Tabbagh [b], Michel Ritz [a]

[a] *IRD, Laboratoire de Géophysique, 32 avenue H. Varagnat, 93143 Bondy Cedex, France*

[b] *Département de Géophysique Appliquée, UMR 7619 Sisyphe, Université Pierre et Marie Curie, case courrier 105, 4 place Jussieu, 75252 Paris Cedex 05, France*

Received 24 June 1999; accepted 4 May 2000

Abstract

A Time Domain Electromagnetic (TDEM) survey was carried out in and around the caldera of the Fogo volcano, Cape Verde Islands, to detect the low resistive structures that could be related to groundwater. A sign reversal in the sounding curves was encountered in central-loop measurements for the soundings located in the centre of the caldera along three main radial profiles. The negative transients are recorded in the early channels between 6.8 and 37 μs. Negative values in an early time transient is an unusual field observation, and consequently the first step was to check the data to ascertain their accuracy and quality. In the second step, three-dimensional (3D) effects are evaluated and ruled out in this zone, while an Induced Polarization (IP) phenomenon is observed using Direct Current (DC) sounding measurements. In the third step, the IP effect is called upon to explain the TDEM distortions; a Cole–Cole dispersive conductivity is found to be adequate to fit the field data. However, the more relevant one-dimensional (1D) model is recovered when both central-loop and offset-loop data are jointly taken into account, thus indicating that an effect of dispersive conductivity is necessary to explain the field data. The 1D electrical structure exhibits four layers, with decreasing resistivity with depth. Only the first layer is polarizable and its Cole–Cole parameters are $m = 0.85$, $c = 0.8$ and $\tau = 0.02$ ms for chargeability, frequency dependence and time constant, respectively. However, the Cole–Cole parameters deduced from TDEM forward modelling remain different from those deduced from DC/IP sounding. In this volcanic setting, this IP effect may be caused by the presence of small grains of magnetite and/or by the granularity of effusive products (lapillis). As a conclusion, it is shown that a modelling using different TDEM data sets is essential to recover the electrical structure of this area.

Keywords: Central-loop TDEM; Negative transient; Induced Polarization; Cole–Cole modelling; Fogo volcano

* Corresponding author. IRD, Geophysique BP 182, Ouagadougou, Burkina Faso. Tel.: +226-30-67-37; fax: +226-31-03-85.

E-mail addresses: marc.descloitres@ird.bf (M. Descloitres), albouy@bondy.ird.fr (Y. Albouy), alat@ccr.jussieu.fr (A. Tabbagh), michel.ritz@ird.sn (M. Ritz).

0926-9851/00/$ - see front matter
PII: S0926-9851(00)00015-X

1. Introduction

During the last 20 years, Induced Polarization (IP) effects in Time Domain Electromagnetism (TDEM) have been reported in field surveys. Resulting distortions of the sounding curves cannot be explain by common 1D models, and may lead to erroneous interpretation if the IP effect is not recognised. Among the papers dealing with IP effects, many describe the theoretical and field data obtained using coincident-loop or central-loop configurations. The more severely distorted TDEM curves show negative data at the end of the transients, which are not expected in such geometrical configurations.

Many authors have modelled distorted ground response by frequency-dependent conductivities (Spies, 1980; Lee, 1981; Walker and Kawasaki, 1988; Flis et al., 1989; Kaufman et al., 1989; Smith and West, 1989; Elliott, 1991; El-Kaliouby et al., 1995; El-Kaliouby et al., 1997). The Cole–Cole formula introduces three polarization parameters: the Cole–Cole chargeability (m), the frequency dependence (c), and the Cole–Cole time constant (τ). All studies agree that the Cole–Cole model is adequate to take into account the IP effect observed in TDEM. These procedures are generally motivated by the necessity to (i) recover the true resistivity model of the ground (see, e.g. Flis, 1987 or Hohmann and Newman, 1990 for 3D polarizable bodies), (ii) enhance the IP response in order to better characterise IP target parameters (El-Kaliouby et al., 1995, 1997), (iii) estimate IP parameters of clays in hydrogeological surveys (Everett, 1997). Theoretical papers have also investigated the possible separation between IP and inductive responses. For this purpose, Kamenetsky and Timofeyev (1984) suggested deploying different sizes of transmitter loop in order to provide different data sets used for the modelling. Kaufman et al. (1989) explore the influence of Cole–Cole parameters for three common transmitter–receiver configurations — central-loop, coincident-loop and dipole–dipole. Under certain conditions, they separate the inductive and polarizable parts of the response. Another practical approach is proposed by McNeill (1994) who advocates the use of offset-loop soundings in order to attenuate or even avoid the IP distortions obtained in central-loop configuration. Finally, Kamenetsky and Novikov (1997) propose a physical modelling approach in order to get laboratory measurements on rock samples.

When dealing with the interpretation of distorted TDEM curves using a dispersive model, the interpreter is confronted with many equivalent models. In addition to resistivity and thickness, three unknown Cole–Cole parameters are needed to fit the field data. Some rules have been pointed out when investigating the influence of Cole–Cole parameters upon TDEM curves (Kaufman et al., 1989; El-Kaliouby et al., 1997). Even so, the interpretation is still difficult and does not necessarily lead to an unique model. Consequently, the determination of the resistivities and thicknesses could remain uncertain.

This study was primarily motivated by the need to interpret central-loop data with sign reversal that are obtained when prospecting for aquifers inside the caldera of the Fogo volcano, Cape Verde Islands (Descloitres et al., 1995). For this survey, the distorted transients are unusual because the negatives occur at the beginning of early time portion of the curves. This is contrary to most of the studies previously mentioned, where the negatives occur at the end of the curves, or in the middle of the curves («double sign reversal») as Walker and Kawasaki (1988) or Barsukov and Fainberg (1998) noticed. To the best of our knowledge, an early time sign reversal in a field observation is unpublished. Therefore, the primary purpose of this paper is to present the field data as a case history of negative data in the early part of TDEM transients. The second aim of this paper is to present an explanation of the observation with a model of these data assuming that the negative transient is due to an IP effect using a Cole–Cole dispersive model. We pay particular attention to incorporate multi-loop and offset-

loop data obtained at the same site into the modelling procedure. This allows us to demonstrate that (i) the IP effect is effectively removed or attenuated when larger transmitter loop or offset-loop configurations are used and (ii) multi-data modelling improves the interpretation allowing a better determination of the Cole–Cole parameters as well as the geoelectrical model.

2. Survey setting

The data presented here are a part of a TDEM survey for groundwater carried out inside the caldera of the Fogo volcano. The 25-km-diameter island is an active hot spot of the Cape Verde Islands. This archipelago, 600 km from the coast of west Africa, is semi-desert. The rainfall on Fogo varies between 200 and 1000

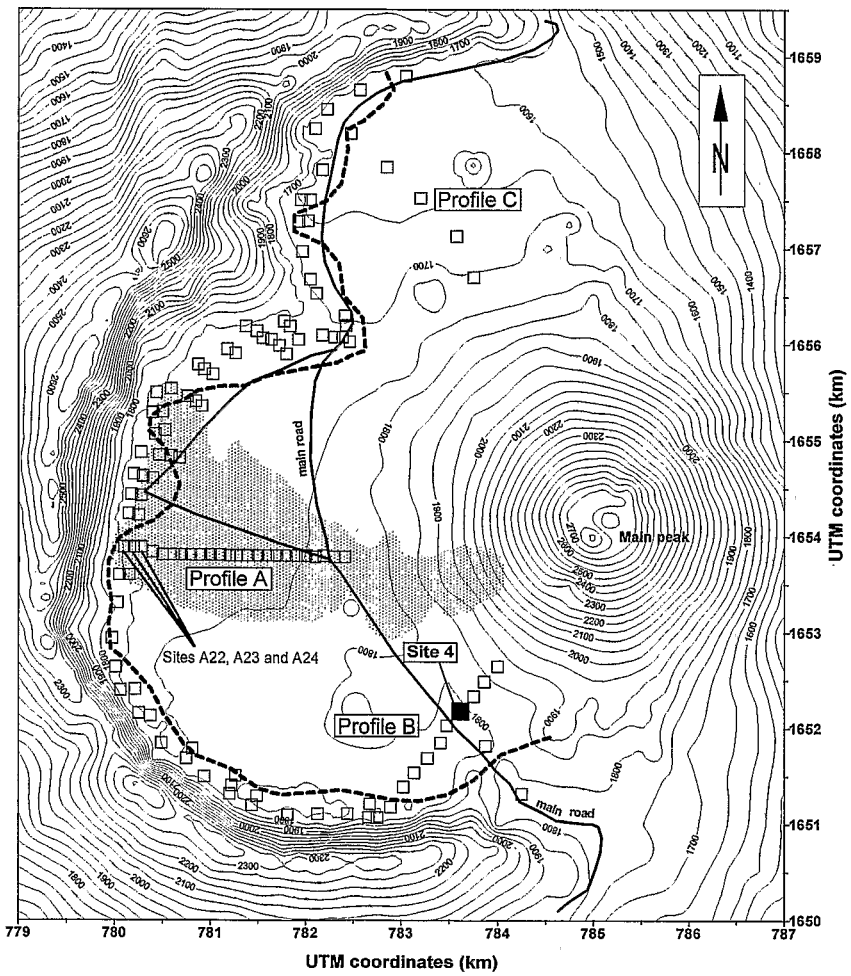

Fig. 1. Topographic map of the caldera and main peak of the Fogo volcano. The location of the TDEM sites are indicated with blank squares (1994 survey). Filled square: test site B4 presented in this study (1995 survey). Area in gray: location of the 1995 lava flows. The dashed line separates TDEM points into two zones: the TDEM curves from points situated between this line and the caldera rim do not show any negative values and detect shallow conductive layers (not presented in this study), and the others, mainly situated along the profiles A, B and C, are similar to site B4 and show negative values.

mm a year in locations related to prevailing winds. The inhabitants are facing with many problems due to insufficient water supply. Rainwater penetrates into the highly permeable surface materials, a phenomenon that leads to crucial irrigation problems. The caldera is a large semi-cylindrical structure 1750 m high bordered to the west by a 500- to 1000-m high wall (Fig. 1). This caldera has a diameter of 8 km and the bottom is a flat terrain considered as the main recharge zone for groundwater (Barmen et al., 1990). The caldera is filled by volcanic products. The surface generally consists in dry pahoehoe and lava flows, lapillis and/or ashes. Geophysics has been considered here in order to detect conductive layers that could be related to groundwater. Previous tests of the audiomagnetotelluric (AMT) method were done. They were unsuccessful principally because of poor AMT signal, strong topographic effects and many difficulties in getting good ground contacts for telluric measurements. TDEM measurements were carried out at the same time, and were found to be more effective.

3. Method and data acquisition

The TDEM method is a controlled source electromagnetic (EM) method that uses a large loop laid on the ground as a transmitter. A current is alternatively turned on and off in the loop. When the current is flowing, a primary static EM field is created. When the current is turned off, an EMF produces eddy currents flowing in the earth, diffusing further into the formation. The eddy currents create a secondary EM field whose amplitude decreases with time. During the absence of current in the transmitter, this EM field due to eddy current in the earth is measured on the surface by a receiver coil. The shape of the decay voltage, or transient, with time depends on the ground resistivity distribution and the array configuration. The transmitter loop can be laid out using various configurations, depending on the objectives of the survey. The most common for shallow applications are the central-loop, coincident-loop and offset-loop modes. For a comprehensive review of the TDEM method, see Nabighian and MacNae (1991) or McNeill (1994).

A Geonics PROTEM 47 system was chosen in our first survey in 1994, because it was easy to handle over difficult terrains. We laid out a 100×100 m^2 transmitter loop for central-loop measurements. A total of 117 soundings sites were covered within 17 days. They are located along three main radial profiles and the contours of the caldera (Fig. 1). The distorted TDEM curves are mainly located along the three profiles. A second survey dedicated to the study of the distorted transient was carried out in 1995. Both EM 47 and 37 systems were deployed on the test site B4 located in the south of the caldera (Fig. 1), which was the only accessible place after the eruption of the volcano in April 95.

The PROTEM system allows TDEM data to be acquired using several base frequencies. Each frequency-based acquisition typically result in 20 normalized voltages logarithmically spaced in time. For EM 47, two overlapping base frequencies were recorded — «u» 237.5 Hz and «v» 62.5 Hz, with time sampling from 6.8 μs to 2.79 ms. The EM 37 system has a higher transmitter voltage, and two overlapping base frequencies were recorded — «H» 25 Hz and «M» 6.25 Hz, with time sampling from 88 μs to 27.8 ms. For the last channels of the «M» base frequency and the large transmitter moments, measurements show that the noise level is reached. The following measurements were made on site B4:

- central-loop measurements using four different square transmitter loops: 100×100, 200×200, 300×300 and 400×400 m^2;
- offset-loop measurements using 100×100 m^2 transmitter loop and 100, 150 and 200 m offsets;
- measurements of the primary field along a profile crossing a 100×100 m^2 loop, and

measurements of three component of the time-varying secondary magnetic field have been performed in order to evaluate if any 2D or 3D structures occur beneath this site.

In order to complete our study of site B4, Direct Current (DC) and time domain IP Schlumberger soundings were carried out using a SYSCAL-R2 resistivity-meter from IRIS Instruments.

4. Field data at site B4

4.1. Central loop TDEM data

The data for site B4 are presented in Fig. 2 as normalized voltage vs. time for overlapping «u», «H» and «M» base frequencies. The «v» base frequency is omitted here to simplify the figure.

For 100×100 m^2 data recorded at «u» base frequency, the first eight channels show negative data from 6.8 to 37 μs; the other 12 channels remain positive. For the 200×200 m^2 data, only the first two channels are negative.

For all of the curves recorded at «H» and «M» base frequencies, as well as for 300×300 and 400×400 m^2 transmitters, there are no negative data.

It should be noted that negative responses occur in the early part of the decay, before 37 μs, and would not have been observed with any TDEM equipment starting acquisition 37 μs after the turn-off time. Furthermore, the negative part of the signal is less important or van-

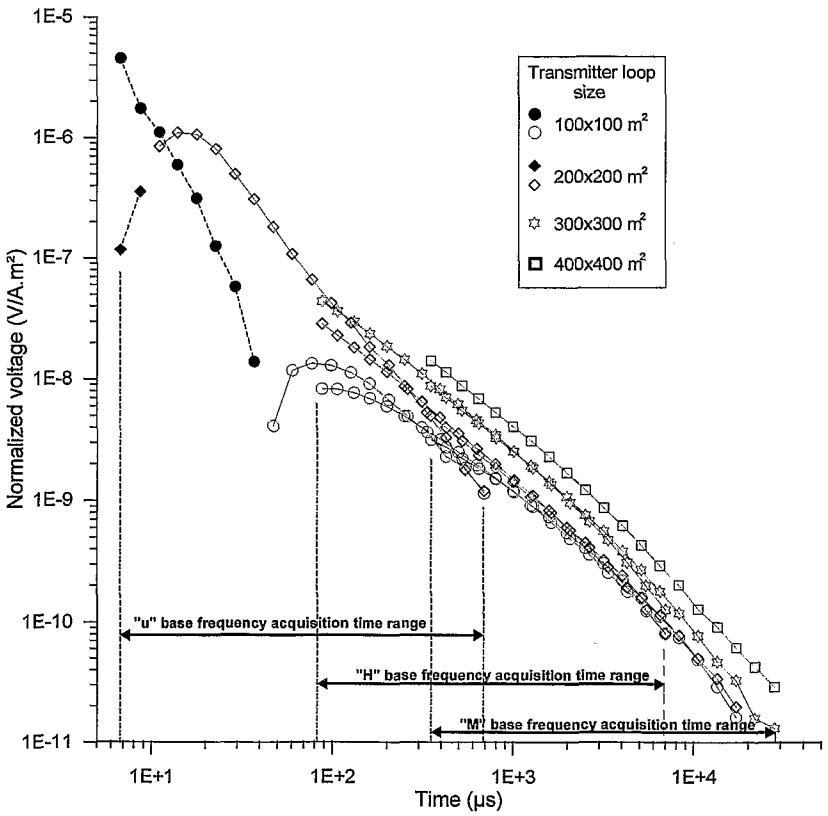

Fig. 2. TDEM central-loop field data measured at site B4. The «u» base frequency transients are provided by an EM 47 system, while «H» and «M» base frequency transients are provided by an EM 37 system. The filled symbols and dashed lines indicate negative values, blank symbols and continuous lines are positive values.

ishes when larger transmitter loop or offset-loop configurations are used.

4.2. Offset-loop and 3D TDEM data

Offset-loop measurements were acquired at the four cardinal points from the cable, at offsets of 100, 150 and 200 m. Fig. 3 presents the 100 m offset curves west and east of the 100 × 100 m^2 loop transmitter. Those curves are close together and always positive.

For the 3D measurements, the X and Y components measured at the centre show that transient levels remain one decade below the Z component level and fall into EM and instrumental noise between 100 and 300 μs.

According to offset-loop measurements, there is no evidence of 3D structure beneath this site that would explain central-loop TDEM distortions.

4.3. DC and IP Schlumberger soundings

Both DC and IP Schlumberger soundings reveal (i) a decreasing apparent resistivity curve from 15,000 to 5000 Ω m for an AB/2 length of 200 m and (ii) a decreasing IP apparent chargeability curve from around 30 to 10 mV/V. The weighted average of the apparent chargeability is calculated with the four registered time windows, ranging from 160 to 1580 ms after the current turn-off. The evidence of a

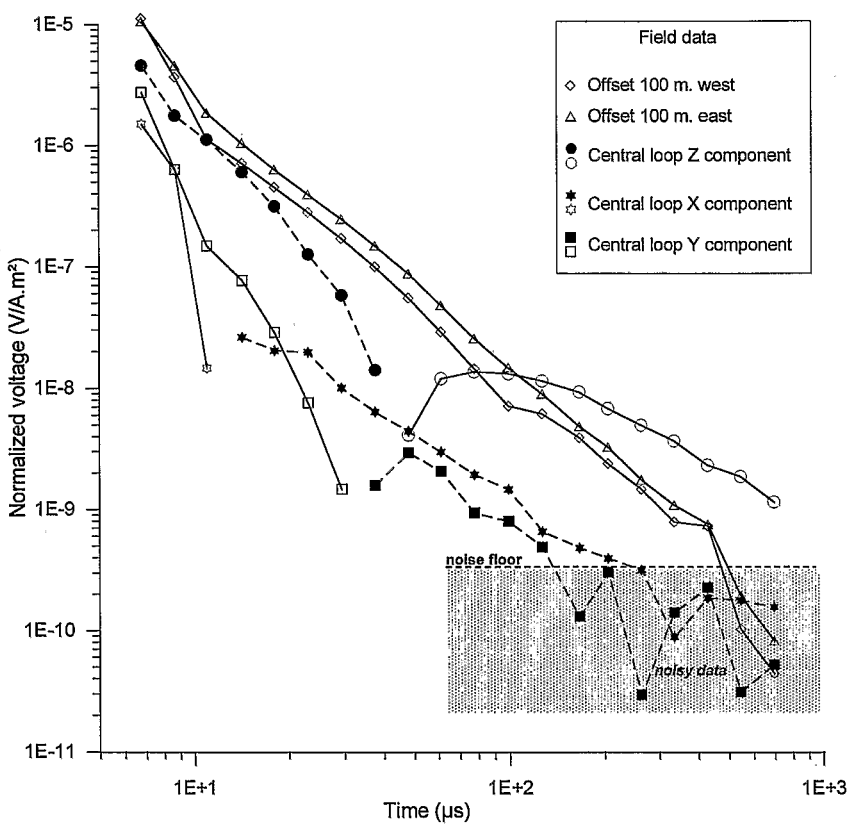

Fig. 3. TDEM offset-loop and 3D central-loop field data measured at site B4 at «u» base frequency. The filled symbols and dashed lines indicate negative values, blank symbols and continuous lines are positive values. North and south offset-loop data as well as 150 and 200 m offset data are omitted here for clarity, and remain identical to the west and east transient. The X component is oriented to the north.

time domain electrical IP response in such ground is an indication to consider an IP effect to explain the distortions of TDEM curves in an earlier range of time.

5. Quality control of the data

As already noted, the occurrence of negative data in the first part of a central-loop transient has never been reported in published papers. Therefore, it is logical to suspect any problem linked to acquisition process that could produced such distortions. Below, we evaluate possible field errors or instrumental problems: the inversion of the polarity, a non-synchronous acquisition or inappropriate receiver bandwidth, and a transmitter, i.e. turn-off effect.

5.1. Control of the polarity of the data

The data acquired in 1994 at the three adjacent sites A22, A23 and A24 at the west end of profile A (Fig. 1) are presented in Fig. 4a. At these sites, the duration of the negative part of the transient reduces itself when the loop is moved closer to the rim. At site A24, the curve remains entirely positive. This shows a progressive attenuation or even the disappearance of the phenomenon and ascertains that the sign of the responses are correct, i.e. that the negatives are present in the first part of the transient.

To reinforce this assertion, Fig. 4b shows the shape of the primary field recorded at several locations of the receiver moving across the 100 $\times$ 100 m^2 transmitter loop at site B4. The theoretical primary field is also calculated for this loop. It remains close to the field data. According to Lenz law for central-loop acquisition, the sign of the primary field is identical to the sign of the secondary field when the measurements are made after a current turn-off. In our case, the primary field remains positive in the centre of the loop while the first measured windows exhibit negative values. This fact leads us to the same conclusion, i.e. that the negative values observed in central-loop data cannot be due to any mistake in the polarity of connections.

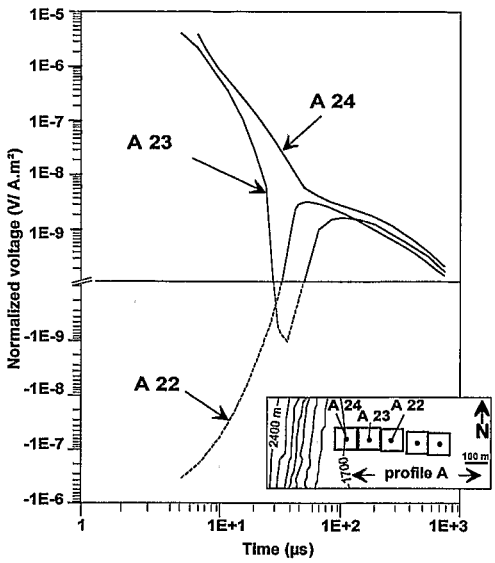

a) Transients recorded at the west end of profile A at "u" base frequency.

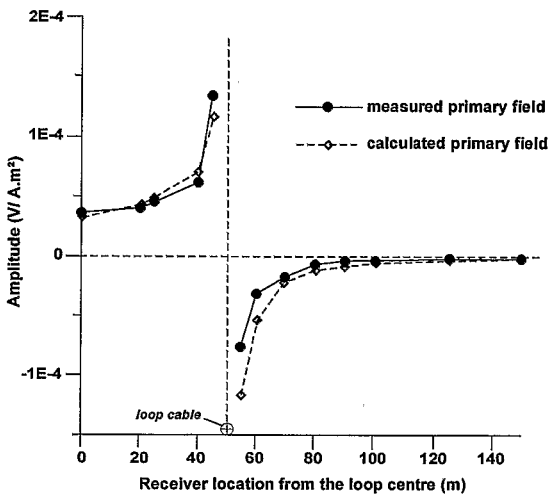

b) Measured primary field at site B4 and calculated primary field for a 100 x100 m² transmitter loop.

Fig. 4. (a) Example of three sounding curves obtained at the west end of profile A with 100$\times$100 m^2 central-loop array configuration. (b) Comparison between the primary field measured at site B4 and the primary field calculated for a 100$\times$100 m^2 transmitter loop for different locations of the receiver coil crossing the loop.

5.2. Non-synchronous acquisition or inappropriate receiver bandwidth

Improper timing of the acquisition could lead to the fact that the first windows of the transient should have been registered during the turn-off of the primary signal. In the same way, a limited receiver bandwidth could integrate the receiver response to the primary field so it extends into the time window of early measurements. As told above, for a central-loop acquisition, the primary and secondary fields should have the same polarity after a current turn-off. Therefore, any synchronisation problem locating the acquisition time into the turn-off time should only manifest itself by an increasing amplitude of early time positive measurements, but never in reversing their polarity. In the case of limited receiver bandwidth, the effect is to delay the response, but never to reverse the sign (Geonics, pers. comm.). This fact is confirmed by Effersø et al. (1999).

5.3. Transmitter turn-off effect

In high resistive ground conditions, the response of the transmitter loop to an abrupt turn-off time (5.2 μs in a 100×100 m^2 loop) could lead to an improper shape of the current ramp, which exhibits some oscillations around zero, as shown in Fig. 5. If such a condition

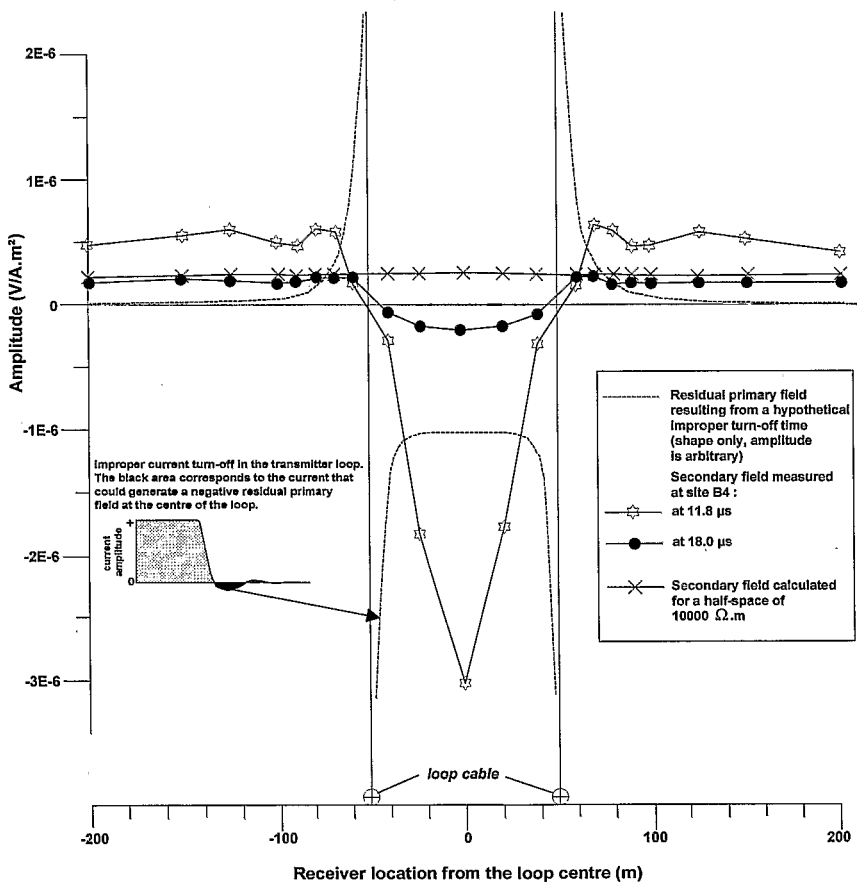

Fig. 5. Comparison between the shapes and the signs of: (i) the secondary field measured at site B4 for two time windows of 11.8 and 18 μs, (ii) the secondary field calculated for a half-space of 10,000 Ω m, and (iii) the residual primary field resulting from a hypothetical improper turn-off time for different receiver locations crossing the 100×100 m^2 transmitter loop. Symbols have been linked here with continuous lines for visual clarity.

exists, a residual primary field with opposite polarity could be present at the end of the ramp leading to the following remark: if a negative response observed in the central-loop is due to residual negative current flowing into the transmitter loop in reaction to an improper turn-off, there should exists a strict amplitude relation between this signal and the signal observed at the different offset locations. This residual signal in offset should indeed have the same variation in time, an inverse polarity, i.e. positive if the signal at the centre is negative, and a decreasing amplitude when the offset distance increases.

For further illustration, we have drawn in Fig. 5 the amplitude of the transient vs. the receiver location for the time windows at 11.8 and 18 μs. Inside the transmitter loop, where the residual primary field is supposed to be negative, the sign of the secondary field is also negative, but their shapes are not the same. Outside the transmitter loop, the signs remain identical, but again their shapes are not the same; the amplitude of the primary field decreases abruptly with increasing distance, while the secondary field is increasing at the same time to reach an amplitude relatively constant in accordance with normal behaviour, as shown as an example for the calculated response over a half-space of 10,000 Ω m.

These results indicate that the negative secondary field in the centre of the loop cannot be related to any residual negative current flowing into the transmitter loop.

6. Data modelling

The occurrence of an IP signal in conventional DC/IP sounding, as well as the progressive disappearance of negative transients when larger transmitter loop central-loop or offset-loop configurations are used, leads us to attempt forward modelling of the data with Cole–Cole dispersive conductivity.

6.1. Some aspects of TDEM 1D modelling using Cole–Cole parameters

The influence of IP effects on TDEM curves is mostly discussed for the coincident-loop configuration (Kaufman et al., 1989; El-Kaliouby et al., 1997) and sometimes for the central-loop (Elliott, 1991) or offset-loop soundings (Everett, 1997). These publications use the Cole–Cole model (Cole and Cole, 1941; Pelton et al., 1978). The formulation expresses the ground conductivity as a dispersive (frequency-dependent) conductivity σ:

$$\sigma = \sigma_0 \frac{1 + (i\omega\tau)^c}{1 + (1-m)(i\omega\tau)^c}$$

where σ_0 is the DC conductivity (S/m), m the Cole–Cole chargeability ($0 \le m \le 1$), c the frequency dependence ($0 \le c \le 1$), τ the Cole–Cole time constant (s), and ω the angular frequency (Hz).

Among many results provided by the aforementioned papers, the following conclusions were obtained for coincident-loop and central-loop configurations in time domain.

- The part of the TDEM response due to the IP effect is negative. In some situations, when the amplitude of the inductive part of the response becomes small enough, the IP signal dominates and leads to negative data. This occurs usually at late time.
- The more resistive the ground, the higher the amplitude of the IP effect. In general, it can be shown that the amplitude of negative peaks is roughly proportional to the square root of the resistivity.
- When sign reversal are recorded, the time of occurrence and amplitude of the negative peak are strictly connected with the value of m, c and τ.
- It is found that the amplitude of the negative part of the total response is roughly proportional to the loop radius while the inductive part of the total response increases as the square of the radius. The larger the transmitter loop, the less predominant the IP effect should be. It is

described by Kaufman et al. (1989) for central-loop systems. El-Kaliouby et al. (1997) determine an optimum loop radius to enhance the amplitude of the phenomenon for coincident-loop system over a polarizable half space. This leads to a better determination of the Cole–Cole parameters of the target.

For a defined polarizable model, these studies point out that the transmitter–receiver configuration governs the shape and the amplitude of the IP effect.

6.2. Forward modelling of the TDEM data using Cole–Cole parameters

The 1D code we used for magnetic TDEM response forward modelling (Tabbagh and Dabas, 1996) was modified to take into account a Cole–Cole conductivity behaviour. For each layer, the conductivity can be complex and is described by the Cole–Cole formula. The current turn-on and turn-off times are described by considering a series of successive step functions to follow the Geonics current waveform. The calculation of the transient response is provided either at the centre of the transmitter loop or at any offset location, and is given for the Geonics-defined time windows.

The Cole–Cole forward modelling of the 100 $\times$ 100, 200 $\times$ 200 m^2 central-loop and 100 m offset-loop data at «u» base frequency is presented in Fig. 6. First, we tried to fit the 100 $\times$ 100 m^2 central-loop data: a preliminary model, A, consists in a two-layer structure with the first layer having a resistivity ρ of 10,000 Ω m and 200 m thick and its Cole–Cole parameters are $m = 0.65$, $c = 0.5$ and $\tau = 0.1$ ms. The second layer is conductive of $\rho = 250$ Ω m and non-polarizable. The model fits the 100 $\times$ 100 m^2 central-loop data with a good agreement. The voltage response for the model A is then calculated for 200 $\times$ 200 m^2 and 100 m offset data. It is quite different from the field data. Hence, the model A cannot be considered as relevant, because it fits only the 100 $\times$ 100 m^2 central-loop data. Therefore, we decided to take into account

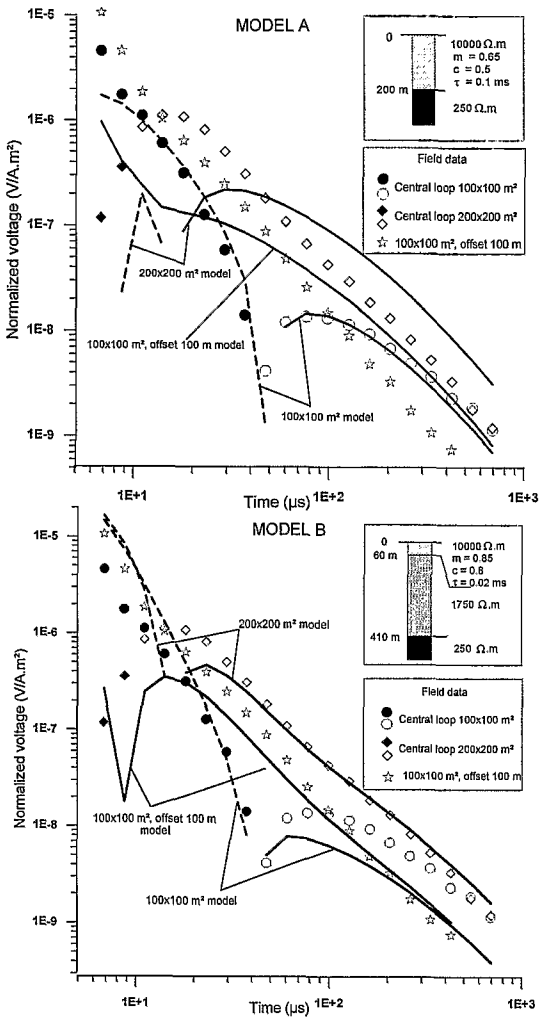

Fig. 6. Cole–Cole forward modelling of «u» base frequency transients for 100 $\times$ 100, 200 $\times$ 200 m^2 central-loop and 100 m offset field data. The filled symbols and dashed lines indicate negative values, blank symbols and continuous lines are positive values. The lines are the resulting calculated transients for model A and B.

larger loop sizes and offset-loop data to improve the model.

In a second step, following McNeill (1994), we consider that the 100 $\times$ 100 m^2 offset-loop data of should be less affected by the IP effect: the 100, 150 and 200 m offset data are indeed free from any negatives. The inversion is done using TEMIX Interpex software for a 1D layered earth with the minimal number of layers required for a correct fitting. This inversion is

illustrated in Fig. 7 for «u» base frequency acquisition. For the three sets of offset-loop data, the models are almost identical and equivalence analysis determines an average three-layer model showing:

1. a resistive, 3000–70 000 Ω m, first layer of 35–90 m thick;
2. an intermediate resistive, 1700–2200 Ω m, second layer of 370–420 m thick;
3. a low resistive, 190–600 Ω m, basement.

In a third step, this three-layer solution was taken as a starting solution for a forward modelling of the central-loop data including Cole–Cole parameters. After some trial and error, the model B shows:

1. a resistive, polarizable first layer of 60 m thick, with resistivity of 10,000 Ω m and Cole–Cole parameters of $m = 0.85$, $c = 0.8$ and $\tau = 0.02$ ms.
2. a second non-polarizable layer, with a resistivity of approximately 1750 Ω m and thickness of about 350 m; and
3. a non-polarizable conductive layer of 250 Ω m resistivity.

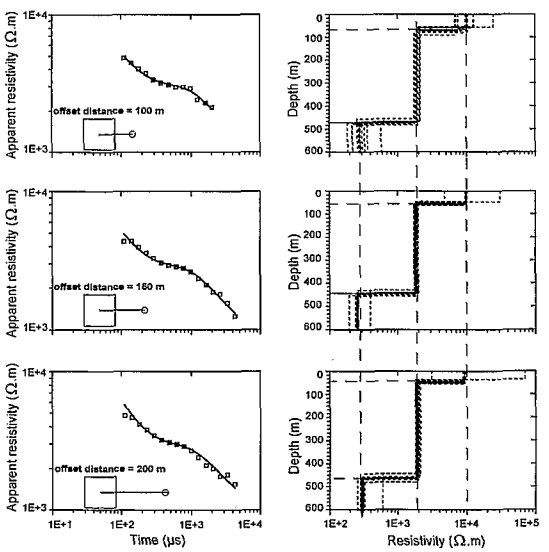

Fig. 7. 1D inversion of the data acquired at site B4 with «u» base frequencies for offset distances of 100, 150 and 200 m from the centre of the 100×100 m^2 transmitter loop. The inversion is made using TEMIX software. The averaged model deduced from these inversions is used as a starting solution in Cole–Cole forward modelling resulting in model B (see text).

In Fig. 6, the resulting curves for 100×100, 200×200 m^2 central-loop and 100 m offset-loop configuration are presented. For the 100×100 m^2 central-loop configuration, model B does not fit the field data as well as model A did, but the amplitude of the negative part and time of sign reversal fits the data reasonably well. For the 200×200 m^2 central-loop and offset-loop configurations, the resulting curves of model B fit the field data reasonably well. Attempts have been made to improve the fit of the last part of the 100×100 m^2 field data and to evaluate the equivalence ranges of the Cole–Cole parameters. If their values are changed more than 5–10%, the resulting synthetic transients do not fit any of the three TDEM field data sets. This confirms that the use of different data sets improves the definition of the model as was already pointed out by Krivochieva and Chouteau (1997) for a non-dispersive medium. It is found to be the case also in dispersive medium.

At this stage, model B appears to be more relevant than model A, even if its fit remains imperfect to the late part of the 100×100 m^2 central-loop data. The following observations are to be noted.

- The Cole–Cole modelling allows the recovery of a transient shape close to the field data, including negatives in the first part of the transients, provided that high values of chargeability and frequency dependence, as well as short time constant, are chosen. This does not necessarily proves that an IP effect is the only possible explanation for the sign reversal, but shows that an IP effect cannot be ruled out to explain the sign reversal phenomenon.
- Model A shows a conductive layer of 250 Ω m at a depth of 200 m. The more relevant model B shows a conductive layer of 250 Ω m at a depth of 410 m. It is shown that if a unique set of data, i.e. 100×100 m^2 central-loop, is

used to model the data, a severe misinterpretation can occur.

• The resistivities and thicknesses deduced from non-dispersive 1D inversion offset-loop data remain close to those calculated with Cole–Cole forward modelling (model B). This tends to confirm that offset-loop data are less affected by any IP effect.

6.3. Interpretation of 300 × 300 and 400 × 400 m^2 central-loop low base frequency data

In order to validate the presence and the depth of the conductive layer in this part of the caldera, we have conducted a 1D inversion using 300 × 300 and 400 × 400 m^2 central-loop data at «H» and «M» base frequencies.

A forward calculation of the dispersive model B was computed for both configurations. The results show that the presence of the first polarizable layer does not significantly modify the transient response for time windows between 88 μs and 2.79 ms. This confirms that, for model B with late transient and larger transmitter loop, the inductive part of the response is much more predominant than the polarizable part of the response originated by the first layer.

These results allow us to conduct a 1D inversion, presented in Fig. 8 as apparent resistivity vs. time for «H» and «M» base frequencies. Using model B as a starting solution for upper layers, but without any Cole–Cole parameters, a fourth layer has been added in order to fit the data and results in model C as follows:

Layer	Resistivity range (Ω m)	Thickness (m)
1	10,000 (fixed)	60
2	1800–4000	300
3	150–250	230
4	50	–

Model C confirms the presence of a conductive layer of 150–250 Ω m at a depth of 360 m, which is close to the model B solution of 250 Ω m and 410 m deep. Moreover, this inversion defines a fourth layer more conductive (50 Ω m) and at a depth of 590 m, which could not

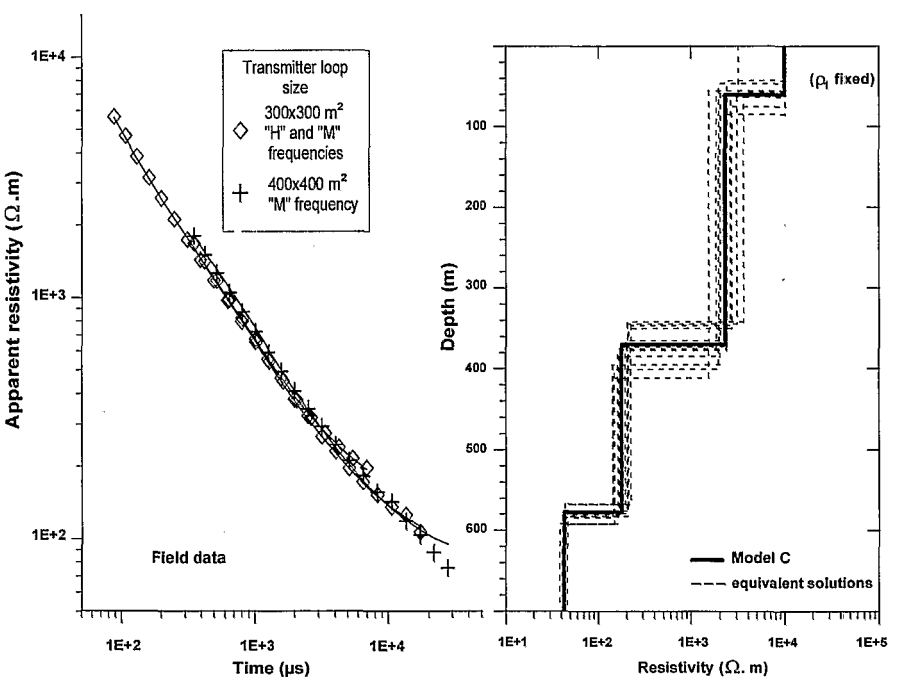

Fig. 8. 1D inversion of the data acquired with «H» and «M» base frequencies for 300 × 300 and 400 × 400 m^2 central-loop data using TEMIX software. Apparent resistivity vs. time field transients are plotted on the left. Model C is represented on the right side with equivalence solutions.

logically be determined by higher base frequency transients.

6.4. Modelling of DC / IP sounding data

In order to detail the uppermost part of the geoelectrical section where model B describes a resistive polarizable layer of 60 m thick, we have carried out a joint inversion of DC and IP sounding data using the software of Sandberg (1993). The results are presented in Fig. 9. The resulting model D consists of a three-layer structure as follows:

Layer	Resistivity (Ω m)	Thickness (m)	chargeability (mV/V)
1	14,790	5.7	28
2	8620	24	18
3	3700	–	11.5

This joint inversion details the upper part of the geoelectrical structure and the first layer of model B and C (10,000 Ω.m, 60 m thick) into three resistive layers. The values of IP chargeability are decreasing regularly with depth. An attempt have been made to transform the raw chargeability data (mV/V) for the four time windows obtained for AB/2 length of 10 m into Cole–Cole parameters using a software developed by IRIS Instrument for the SYSCAL R2 data. For a fixed frequency dependence (c) of 0.8, the chargeability (m) and the time constant (τ) are 0.06 and 1.16 s, respectively. Those results have to be taken with caution because the raw data are measured over only four time windows with this equipment, which gives a poor sampling of the IP transient decay. Even with this precaution, those values are far from $m = 0.85$ and $\tau = 0.02$ ms deduced from TDEM forward modelling in model B.

6.5. Final model

Forward Cole–Cole modelling (model B), inversion of large loop TDEM data (model C)

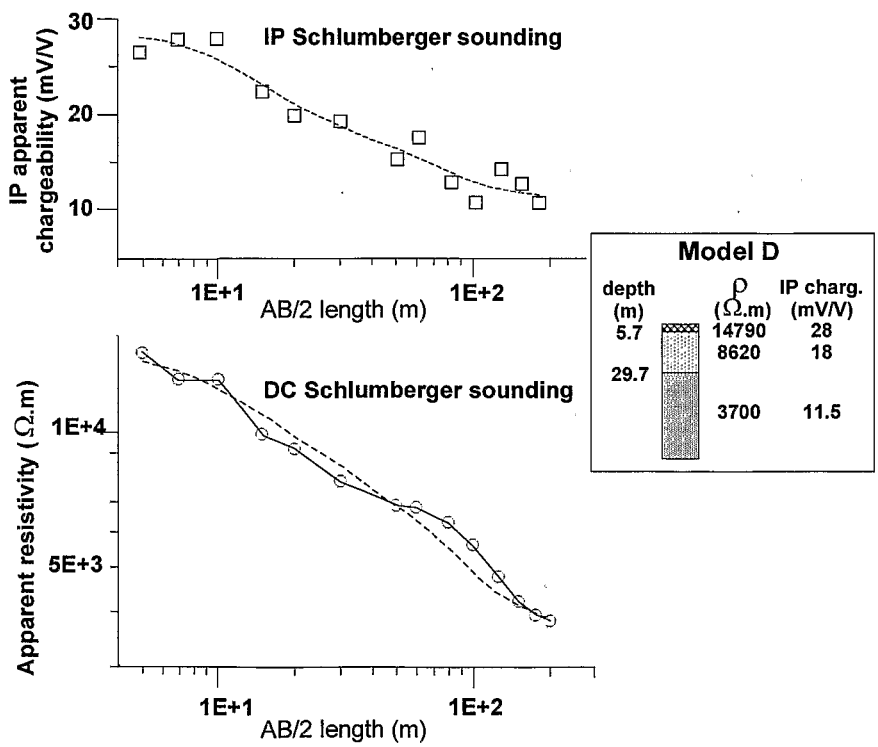

Fig. 9. Joint inversion of DC and time domain IP Schlumberger soundings using the Sandberg software (1993). The dashed lines are calculated from model D.

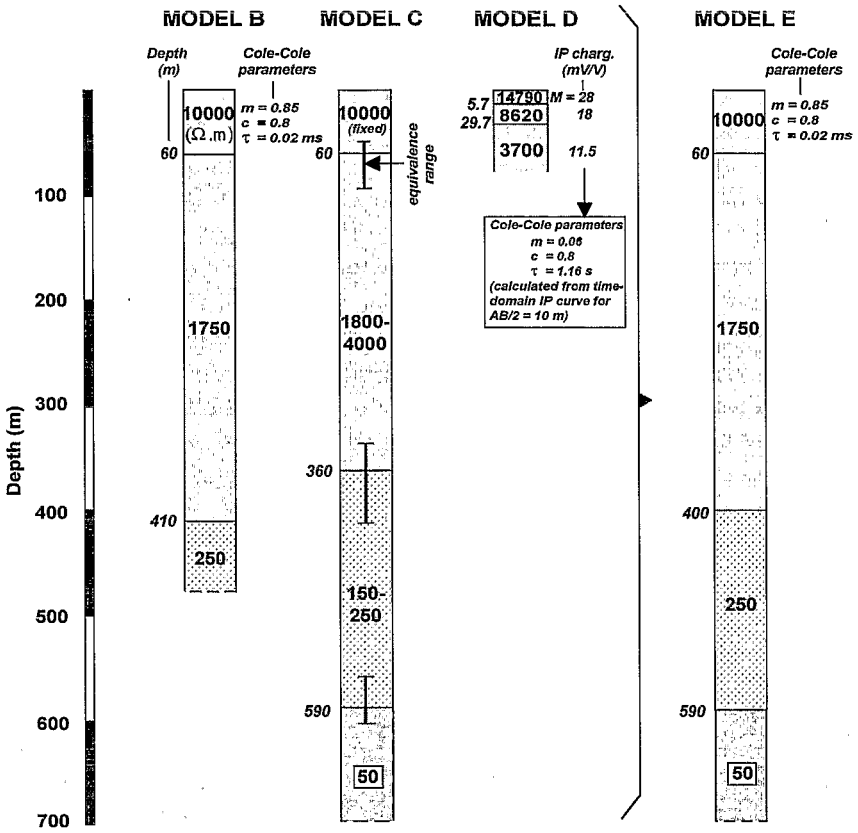

Fig. 10. Comparison between models B, C, D and E. Model B is from Cole–Cole forward modelling of 100×100, 200×200 m^2 central-loop and offset-loop TDEM data with «u» base frequency. Model C is from 1D inversion of 300×300 and 400×400 m^2 central-loop TDEM data with «H» and «M» base frequencies. Model D is from joint inversion of DC and IP Schlumberger soundings. Model E is an average model derived from models B and C, which can be proposed as the resistivity structure below site B4 — results from model D only detail the shallower part of the first resistive layer and are omitted in model E.

and joint inversion of DC/IP data (model D) are presented in Fig. 10. An average model, E, can be derived taking into account the information given by these models. The first layer has a resistivity of 10,000 Ω m, is 60 m thick, and remains the only polarizable layer. Its Cole–Cole parameters deduced from TDEM Cole–Cole forward modelling are $m = 0.85$, $c = 08$ and $\tau = 0.02$ ms. The interpretation of' the DC sounding divided it into three layers with resistivity and thicknesses of 14,790 Ω m, 5.7 m thick, 8620 Ω m, 24 m thick and 3700 Ω m; and IP chargeability of 28, 18 and 11.5 mV/V, respectively of depth. The second layer is less resistive (1750 Ω m) and 340 m thick. The third layer is conductive (250 Ω m) and 190 m thick. The ultimate layer is conductive (50 Ω m) and is only revealed by large transmitter loop TDEM data.

7. Discussion

The first point to be discussed is our approach to model TDEM data using a dispersive conductivity. Once the quality of the data has been ascertained, three main considerations are used to justify such modelling attempt: (i) the occurrence of negative values in central-loop TDEM transients, commonly modelled using

Cole–Cole formula as reported in the literature; (ii) the accordance of the raw TDEM data set to theoretical studies, which mention the attenuation of the IP effect when larger transmitter loop or offset-loop configuration are used; and (iii) the occurrence of IP signal measured in conventional DC/IP sounding. The forward modelling has shown that model B describes the distorted transients, and moreover satisfies the predicted behaviour when multi-data sets are taken into account. Thus, we believe that dispersive conductivity is a possible explanation for our distorted transients. However, parametrization of conventional IP chargeability data obtained with the Schlumberger sounding into the Cole–Cole formulation fails to reconcile the values of m and τ with their corresponding values deduced from TDEM forward modelling. At this stage of the study, we believe that this discrepancy cannot be explained in a simple manner with such data set. But this is not surprising due to the difference in time constants between conventional IP and TDEM, which leads us to the second point of our discussion related to the origin of the IP effect in a volcanic setting.

According to the work on spectral IP by Pelton et al. (1978), it is possible to encounter high chargeabilities m (> 0.8) and short time constant τ (< 0.1 ms) with rocks containing more than 20% of sulfides and a grain size less than 0.1 mm. Moreover, one sample of magnetite from Iron Mount, UT, USA, exhibits a chargeability near 1.0 and a time constant near 0.08 ms. Another example of high chargeability (0.5) and short time constant (0.69 ms) has been calculated from distorted central-loop TDEM measurements for resistive permafrost formation of 1000 Ω m by Walker and Kawasaki (1988). In our case, the origin of the IP effect has to involve dry lapillis and massive lava flows formation. To the best of our knowledge, such an IP effect involving TDEM has not been reported yet for volcanic areas. Some TDEM studies over volcanoes have already been carried out (Jackson and Keller, 1972; Jackson et al., 1986; Fitterman et al., 1988). These studies did not take note of negative voltage in TDEM data, but the transients were recorded at times of a few tens of milliseconds, much later than ours. Patella et al. (1991) describe examples of frequency dispersion in magnetotellurics (MT) data in deep geothermal volcanic zones. The IP effect is attributed to hydrothermal paragenesis, which cannot be taken into account in our shallower case. As clearly described by Flis et al. (1989), the IP effect is generally caused by metallic mineral grains and/or negatively charged clay disseminated in the rock. In our case, we have to rule out the implication of shallow clay layers, which would have been detected in DC sounding as conductive layers. However, the anomalous TDEM soundings are located in our study over thicknesses of tens of meters of lapillis. This material can contain small particles of magnetite (< 0.1 mm) and produce an IP effect in the high frequency range. This fact has to be investigated further to be able to confirm this behaviour, and the presence of small particles does not explain the longer time constant of $\tau = 1.16$ s calculated from DC/IP sounding in the lower frequency range. We believed that an IP effect with a longer time constant could be generated by the granularity of the lapillis having grains of more than 1-mm diameter. This raises the question that if two IP effects with two time constants could coexist why have they not been detected by both TDEM or DC/IP soundings? To answer this question, two calculations have been done. The first one is the TDEM response for the dispersive model B, with Cole–Cole parameters of the first layer fixed to the values of $m = 0.06$, $c = 0.8$ and $\tau = 1.16$ s, deduced from DC/IP sounding. The TDEM response does not differ from a non-dispersive case, that indicates that 100×100 m^2 central-loop high base frequency TDEM acquisition is not sensitive to such small chargeability and long time constant. The second calculation is the response of SYSCAL R2 equipment when the measurements are done over a medium with Cole–Cole parameters deduced from TDEM forward mod-

elling (model B). For the four time windows, the IP response remains near 0.01 mV/V, below the practical measurable amplitude (Iris Instruments, pers. comm.). Those calculations show that if two IP effects could coexist the shorter one is only revealed by the EM 47 equipment and the longer one by the DC/IP SYSCAL R2 instrument.

It should be noted here that normal transients, i.e. positive values, have been recorded in other places of the volcano, where lapillis could also be present, and consequently the exact origin of the IP effect cannot be ascertain with our data set alone and would require laboratory work on rock samples.

The third point of our discussion refers to other possible causes of distorted transients linked with (i) displacement currents and (ii) magnetic viscosity.

Displacement currents are usually neglected in conventional modelling. But when an imaginary part is considered for σ, a corresponding permittivity ε is implicitly considered and the true permittivity effect remains negligible against the imaginary part of the conductivity effect: the results of the forward modelling using dispersive model B and a dielectric constant of 3 for the first layer does not show any difference compared with the $\varepsilon = 0$ case for transients measured 6.8 μs after the current turn-off time.

Magnetic viscosity effects in TDEM data are largely documented in archaeological prospection (Colani and Aitken, 1966a; Mullins and Tite, 1973; Dabas and Skinner, 1993) and also in mining prospection (Buselli, 1982; Spies and Frischknecht, 1991). This phenomenon leads to late time distortion, but never reverses the sign of central-loop or coincident-loop data. We believe that this phenomenon can be ruled out to explain our sign reversal.

The last point to be discussed here is the geological implications of the average model E. As no drilling information is available in this area, we should note that the general resistivity structure is noticed in other studies. Fitterman et al. (1988) has encountered resistive first layers over deep conductive zones in the Newberry volcano. On the flanks of Piton de la Fournaise volcano (Reunion Island), moderately deep 300–500 m conductive layers have been detected and attributed to aquifers and clayey formations (Descloitres et al., 1997). For the averaged model E derived in this study, the resistive first and second layers are attributed to recent dry volcanic formations of basaltic lava, lapillis or ashes. The third intermediate-resistivity layer is attributed to partially or totally water-saturated volcanic rocks alone or those associated with clayey layers between fractured lava flows. The conductive basal layer is attributed to the old volcanic complex-clayey zone related to deep alteration of the volcanic rocks and/or hydrothermal zone.

8. Conclusions

Recording negative data with the TDEM central-loop configuration should lead to suspect an IP (dispersive conductivity) effect. Therefore, to be able to quantify and model the TDEM response, we acquired data using several transmitter loop sizes as well as different positions of the receiver coil.

For shallow applications in case of highly resistive polarizable superficial formations, particularly in such volcanic setting, central-loop measurements using small transmitter loops, i.e. $\leq 100 \times 100$ m^2, should be avoided. The offset-loop data as well as larger loop size measurements are less affected by IP effects. A Cole–Cole model compared to only one set of data can lead to severe misinterpretation. Consequently, in order to be able to get a more relevant model, one should acquire several field data set of different loop sizes and/or offset locations and incorporate them into the modelling. In our case a relevant dispersive model was found (i) using a starting model given by non-dispersive 1D inversion of offset-loop data

and (ii) Cole–Cole modelling through trial and error of central-loop and offset-loop data using various transmitter loop sizes. This procedure greatly improves the determination of resistivity, thickness and Cole–Cole parameters.

Regarding our survey, TDEM method was found to be an adequate way of prospecting low resistivity zones in such volcanic settings but the IP effect detected in some places can be troublesome when attempting to recover the geoelectrical section. The origin of the IP effect detected in this area remains difficult to determine, but the modelling shows that this effect is related to a shallow resistive layer. Using different data sets, the global electrical structure of the central part of this caldera can be estimated. Cole–Cole forward TDEM modelling remains difficult to practice. Any inversion model of different data sets which takes into account Cole–Cole parameters, should help to recover more relevant solutions. No doubt that in other favorable conditions, AMT soundings or large DC soundings could be jointly interpreted with TDEM data in order to give a more constrained image of the subsurface.

Acknowledgements

This work took place as a part of the GEAQUIF research Program of IRD (Institut de Recherche pour le Développement). The 1995 field campaign was partially supported by the Cap-Verdian Institute INGRH (Instituto Nacional de Gestaô dos Recursos Hidricos) and the Mission de Coopération Française in Praia. We wish to thank the two reviewers as well as N.B. Christensen for their constructive criticisms, M. Chouteau from Ecole Polytechnique de Montréal for providing the EM-37 equipment, H. El-Kaliouby for earlier discussions and suggestions to improve the TDEM Cole–Cole models, M. Goldman and M. Bosnar for fruitful discussions on TDEM IP distortions and P.Valla from IRIS Instruments for his help on the conversion of DC/IP data into Cole–Cole parameters. We are grateful to A. Querido, J. Descloitres and N. Mademba for their field contributions.

References

Barmen, G., Carvalho, V. and Querido, A., 1990. Groundwater-related geological and isotopic investigations on the Island of Fogo. An overview. Lund University and INIT file report, Praia, 72 pp.

Barsukov, P.O., Fainberg, E.B., 1998. Double IP Effect in electromagnetic transients. 14th Workshop on Electromagnetic Induction in the Earth, Sinaia, August 16–22. pp. 97–98, Abstracts, paper 6.4.

Buselli, G., 1982. The effect of near-surface superparamagnetic material on electromagnetic measurements. Geophysics 47 (9), 1315–1324.

Colani, C., Aitken, M.J., 1966a. Utilisation of magnetic viscosity in soils for archaeological prospection. Nature 212, 1446–1447.

Cole, K.S., Cole, R.H., 1941. Dispersion and absorption in dielectrics. 1 — Alternating current. J. Chem. Phys. 9, 341–351.

Dabas, M., Skinner, J., 1993. Time domain magnetisation of soils (VRM), experimental relationship to quadrature susceptibilities. Geophysics 58 (3), 326–333.

Descloitres, M., Ritz, M., Mourgues, P., 1995. TDEM soundings for locating aquifers inside the caldera of the Fogo active volcano, Cape Verde Islands. Proceedings of the 1st Meeting of EEGS European Section, Sept 25–27, Torino. pp. 110–114.

Descloitres, M., Ritz, M., Robineau, B., Courteaud, M., 1997. Electrical structure beneath the eastern collapsed flank of Piton de la Fournaise volcano, Reunion Island: implication to the quest for groundwater. Water Resour. Res. 33 (1), 13–19.

Effersø, F., Auken, E., Sørensen, K.I., 1999. Inversion of band limited TEM responses. Geophys. Prospect. 47, 551–564.

El-Kaliouby, H.M., Hussain, S.A., Bayoumi, A., El-Diwany, E.A., Hashish, E.A., 1995. Effect of clayey media parameters on the negative response of a coincident loop. Geophys. Prospect. 43 (5), 595–603.

El-Kaliouby, H.M., El-Diwany, E.A, Hussain, S.A., Hashish, E.A., Bayoumi, A.R., 1997. Optimum negative response of a coincident-loop electromagnetic system above a polarizable half-space. Geophysics 62 (1), 75–79.

Elliott, P., 1991. An empirical procedure for removal of polarisation effects observed in TEM field data. Explor. Geophys. 22 (4), 575–582.

Everett, M.E., 1997. Transient inductive coupling of loops over near-surface clay-bearing sandstones. 67th Ann. Internat. Mtg. (Dallas, TX, November 2–7), Soc. Expl. Geophys.

Fittermann, D.V., Stanley, W.D., Bisdorf, R.J., 1988. Electrical structure of Newberry volcano, Oregon. J. Geophys. Res. 93 (B9), 10119–10134.

Flis, M., 1987. IP effects in 3D TEM data— theory and case histories. Explor. Geophys. 18 (1), 55–58.

Flis, M.F., Newman, G.A., Hohmann, G.W., 1989. Induced-polarization effects in time-domain electromagnetic measurements. Geophysics 54 (4), 514–523.

Hohmann, G.W., Newman, G.A., 1990. Transient electromagnetic response of superficial, polarizable patches (short note). Geophysics 55 (8), 1098–1100.

Jackson, D.B., Keller, G.V., 1972. An electromagnetic sounding survey of the summit of Kilauea volcano, Hawaii. J. Geophys. Res. 77 (26), 4957–4965.

Jackson, D.B., Frischknecht, F.C., Kauahikaua, J., 1986. Three-layer inversions for 18 TDEM soundings in the cone crater area, SW rift zone of Kilauea volcano, Hawaii. U.S. Geol. Surv. Open-file Rep. 87-76.

Kamenetsky, F.M., Timofeyev, V.M., 1984. Possibility to separate induction and polarization transients. Phys. Earth 12, 89–94, (in Russian).

Kamenetsky, F.M., Novikov, P.V., 1997. A physical study of low-frequency dispersion of rock conductivity in time-domain electromagnetics. Geophys. Prospect. 45 (3), 421–434.

Kaufman, A.A., Geoltrain, S., Knoshaug, R.N., 1989. Influence of induced polarization in inductive methods. Geoexploration 26, 75–93.

Krivochieva, S., Chouteau, M., 1997. Improvement in TDEM interpretations by joint inversion of different data sets. 3rd Mtg. (Aarhus, September 8–11), European Section of Environmental and Engineering Geophys. Soc., Proceedings. pp. 347–350.

Lee, T., 1981. Transient electromagnetic response of a polarizable ground. Geophysics 46 (7), 1037–1041.

McNeill, D.J., 1994. Principles and applications of time domain electromagnetic techniques for resistivity soundings. Geonics, technical note TN 27.

Mullins, C.E., Tite, M.S., 1973. The magnetic properties of soils and their application to archaeological prospecting. Archaeophysika 5, 143–347.

Nabighian, M.N., Macnae, J.C., 1991. Time domain electromagnetic prospecting methods. In: Nabighian, M.N. (Ed.), Electromagnetic Methods in Applied Geophysics. Applications vol. 2 SEG publication, pp. 427–520, Chap. 6.

Patella, D., Tramacere, A., Di Maio, R., Siniscalchi, A., 1991. Experimental evidence of resistivity frequency-dispersion in magnetotellurics in the Newberry (Oregon), Snake River Plain (Idaho) and Campi Flegrei (Italy) volcano-geothermal areas. J. Volcanol. Geotherm. Res. 48, 61–75.

Pelton, W.H., Ward, S.H., Hallof, P.G., Sill, W.R., Nelson, P.H., 1978. Mineral discrimination and removal of inductive coupling with multifrequency IP. Geophysics 43 (3), 588–609.

Sandberg, S.K., 1993. Examples of resolution improvement in geoelectrical soundings applied to groundwater investigations. Geophys. Prospect. 41 (2), 207–227.

Smith, R.S., West, G.F., 1989. Field examples of negative coincident-loop transient electromagnetic responses modeled with polarizable half-planes. Geophysics 54 (11), 1491–1498.

Spies, B.R., 1980. A field occurrence of sign reversal with the transient electromagnetic method. Geophys. Prospect. 28 (4), 620–632.

Spies, B.R., Frischknecht, F.C., 1991. Electromagnetic Sounding. In: Nabighian, M. (Ed.), Electromagnetic Methods in Applied Geophysics. Applications vol. 2 SEG publications, Chap. 5.

Tabbagh, A., Dabas, M., 1996. Absolute magnetic viscosity determination using time-domain electromagnetic devices. Archaeol. Prospection 4, 199–208.

Walker, G.G., Kawasaki, K., 1988. Observation of double sign reversal in transient electromagnetic central induction soundings. Geoexploration 25, 245–254.